Multi-Classifier Tree With Transient Features for Drift Compensation in Electronic Nose

Atiq Ur Rehman, *Member, IEEE*, Samir Brahim Belhaouari, *Senior Member, IEEE*, Muhammad Ijaz, Amine Bermak, *Fellow, IEEE*, and Mounir Hamdi, *Fellow, IEEE*

***Abstract*—Long term sensors drift is a challenging problem to solve for instruments like an Electronic Nose System (ENS). These electronic instruments rely on Machine Learning (ML) algorithms for recognizing the sensed odors. The effect of long-term drift influences the performance of ML algorithms and the models those are trained on drift free data fail to perform on the drifted data. Moreover, the response of an electronic nose system depends on the variable response of the sensors and a delay is expected in reaching a steady state by the sensors. In this paper, these two problems of 'sensors long term drift' and 'delayed response' are solved simultaneously to propose a robust and fast electronic nose system, with following merits: (i) only initial transient state features are used in the proposed system without waiting for the sensors to reach a steady state, (ii) a modified boxplot approach is used to handle noisy/drifted data points as a preprocessing step before the classification setup, (iii) a heuristic tree classification approach with optimized transient features is proposed, (iv) the proposed approach only relies on adapted ML methods contrary to the traditional approaches like system recalibration or sensors replacement for handling sensors drift, and (v) the proposed ML model does not require any target domain data and uses only the source domain data for learning the classifier, opposed to the other ML solutions available in the existing literature. The proposed method is tested using a large scale gas sensors drift benchmark dataset available freely on UCI Machine Learning repository and is found better than the existing state-of-the art approaches with an overall accuracy of 87.34%.**

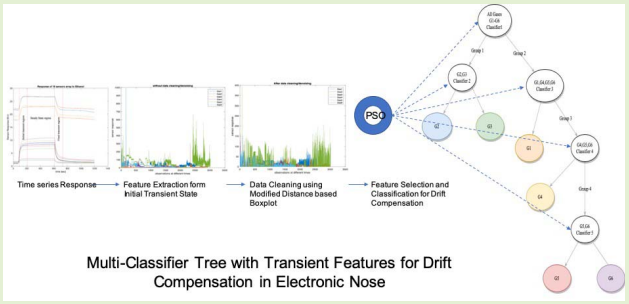

Multi-Classifier Tree with Transient Features for Drift Compensation in Electronic Nose

***Index Terms*— Artificial olfaction, electronic nose, heuristic optimization, industrial gases, sensors drift.**

I. Introduction

ARTIFICIAL Olfaction (AO) refers to identifying and discriminating different odors using electronic instruments like an Electronic Nose System (ENS). The ENS has a broad range of applications including the food industry [1]–[3], health sector [4], [5], environment monitoring [6], oil and gas industry [7], and security purposes [8], [9], among others. An ENS is comprised of two units, a sensing unit and a recognition unit. In the sensing unit, an array of different sensors is used to record the response of different Volatile Organic Compounds (VOCs) and the recorded response is utilized by the recognition unit to identify and discriminate between different VOCs.

Manuscript received November 4, 2020; accepted November 27, 2020. Date of publication December 2, 2020; date of current version February 5, 2021. This work was supported in part by the National Priorities Research Program (NPRP) from the Qatar National Research Fund (a member of Qatar Foundation) under Grant NPRP10-0201-170315 and Grant NPRP11S-0110-180246. The associate editor coordinating the review of this article and approving it for publication was Dr. Sanket Goel. *(Corresponding author: Atiq ur Rehman.)*

The authors are with the ICT Division, College of Science and Engineering, Hamad Bin Khalifa University, Doha 34110, Qatar (e-mail: atiqjadoon@gmail.com; atrehman2@hbku.edu.qa).

Digital Object Identifier 10.1109/JSEN.2020.3041949

Machine Learning (ML) models used in the recognition unit of ENS play a vital role in classifying odors and setting the prediction accuracy of the overall system [10]. However, the performance of these ML models deteriorates due to the gradual occurrence of long-term sensors drift. This happens due to the unpredictable shift in the sensor response data over time and what makes it even more challenging is the fact that the behavior of drift is non-deterministic in nature [11]. Therefore, the models trained on the data that is acquired using new sensors fail to perform when tested on the data acquired using relatively old/used sensors. This means that, for real applications the same device cannot be used for longer periods of time and the system either needs to be recalibrated or requires sensors replacement. Recalibration of system requires a baseline gas that can be used to compensate the drift and sensors replacement/calibration is also associated with an additional cost to the system, which hinders deployment of these sensors outside the Lab and in real-life applications.

Besides the performance of ML algorithms in the presence of drift, another important factor that contributes to the performance of the overall system is response time of the system. The response time of the system is the time a system takes in making a prediction after its exposure to an odor of interest. This response time mainly depends on (i) the response

time of the sensors used in the sensing unit of ENS and (ii) the amount of time ML algorithm takes for computation in the recognition unit. Classical ML algorithms mainly rely on the steady state response of the sensors to discriminate between different odors of interest. The steady state response is also termed as the 'gold-standard' for feature extraction in chemo-sensory community [12]. However, to reach a steady state response the system needs to wait for a very long time (typically in the order of minutes) resulting in unreasonable latency hindering deployment in time-critical applications.

In this paper, the two challenging problems of long-term sensors drift and the large latency of the system are simultaneously solved to propose a fast and robust system, with the following merits:

1) The proposed system does not need to wait for the sensors to reach a steady state, rather it uses only the transient state features to discriminate between different VOCs of interest and it makes the overall response time of the system low, without compromising on the classification accuracy of the system. This makes it suitable for time-critical real applications of ENS.

2) In order to compensate the drift, a novel tree classifier which uses different classifiers at its different nodes is proposed. The nodes of the tree classifier are provided with different heuristically optimized features to discriminate between different VOCs of interest.

3) The proposed solution relies purely on a ML approach and thus it does not require any system recalibration or the sensors replacement for real applications of an ENS.

4) The proposed approach does not require any target domain data for drift compensation as required by other semi-supervised ML solutions proposed in existing literature and relies only on the source domain data for learning the classifier.

5) To the best of our knowledge, this is the first study to test initial transient features for long-term drift compensation in gas sensors.

The proposed technique is tested using a widely used, large size, benchmark dataset for drift and is compared with several existing state-of-art approaches and is found better in terms of classification accuracy with an added advantage of utilizing only the transient state features for a faster response time. The overall classification accuracy achieved is 87.34% which is higher than the existing approaches.

The rest of the paper is organized as follows: Section II (Related work), Section III (Proposed Methodology), Section IV (Performance Evaluation), Section V (Conclusion).

II. Related Work

One of the pioneering works for systematically analyzing the sensors drift in real operating conditions is presented in [13], [14] by Romain *et al.* The authors presented a detailed insight of the sensors drift problem by collecting and analyzing a large dataset over a long period of time. The key conclusions drawn from these studies include the following three points: (i) Metal oxide gas sensors are the best option for long term use, (ii) estimation of drift is recommended using a calibration gas for compensating the drift, and (iii) sensors replacement is considered must for long term use. However, solutions like system recalibration and sensors replacement are tedious and impose an additional maintenance cost.

Other than the solutions listed above, a number of other solutions are also presented in the literature to compensate the drift in sensors. These solutions can be broadly classified as (i) univariate approaches, (ii) multivariate approaches, and (iii) ML approaches [15], [16]. Some examples of univariate approaches are frequency analysis, differential measurement and baseline manipulation [17] whereas, the drawback of these approaches is their sensitivity to sample rate variation [18], [19]. Examples of multivariate approaches include clustering and signal correction [20], [21]. The drawbacks of these approaches are the requirement of frequent sampling and recalibration. ML approaches on the other hand solve the problem of drift by intelligently adapting the model to compensate the drift without any description of the drift.

Some recent ML approaches presented in the scientific literature for drift compensation are mainly based on subspace learning/domain transformations [22]–[24], deep neural networks [25], transfer learning [26], feature selection [27] and semi-supervised learning [16], [28]. Almost all the ML methods presented in literature are able to handle the sensors drift to some extent but still there exists a room for improving the accuracy of these models. Furthermore, these models have some limitations like the computational complexity of the classifiers that contributes to a further delay in the response time of the system, complex hyperparameter tuning, requirement of target domain data for semi-supervised learning and requirement of steady state response of the sensors for better classification accuracy.

X. Pan et al [29] have recently proposed a fast gas recognition system based on a hybrid of convolutional and recurrent neural network that discriminates between different gases based only on the transient features acquired from the beginning of response curve without waiting for the sensors to reach a steady state. The study paves the way to use only transient features for a faster response with high accuracy. However, this study did not consider the effect of long-term sensors drift.

Keeping in view the ability of ML models against sensors drift, with an added advantage of no maintenance cost, this paper proposes a novel tree based classification model with an ability of fast response and robustness again sensors drift. For a better generalization the nodes of the proposed tree based classifier are optimized with a heuristic feature selection algorithm and different classifiers are used at different nodes of the tree for a better classification accuracy. Furthermore, to enhance the response time of the system only transient features acquired at the beginning of the response curve are used for classification.

III. Proposed Methodology

The overall proposed model is based on four stages: (i) feature extraction, (ii) sample cleaning/denoising based on a modified distance based boxplot, (iii) features optimization using an iterative evolutionary feature selection algorithm and (iv) classification using a multi-classifier tree approach. The details of proposed model are given as follows:

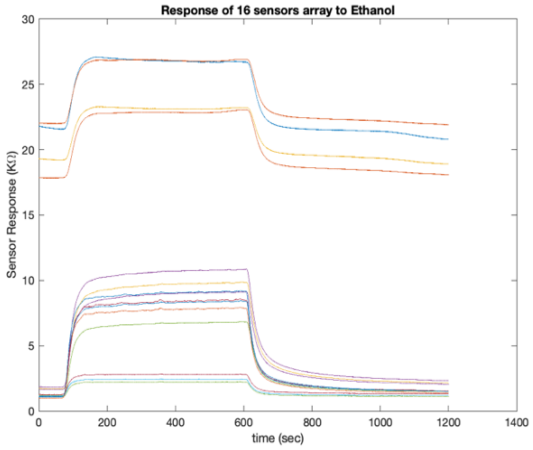

Fig. 1. Response of 16 gas sensors for Ethanol exposure.

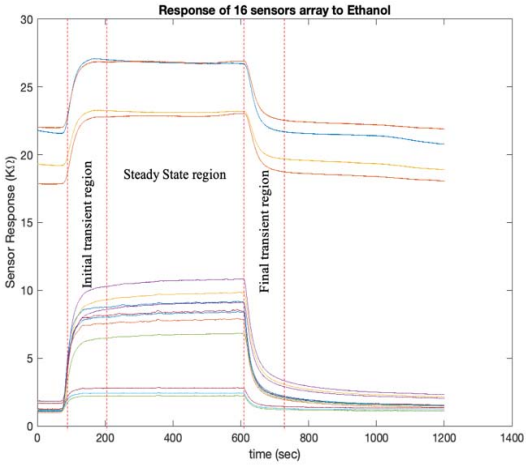

Fig. 2. Three regions of response curve.

A. Feature Extraction

The aim of the study is to utilize only the transient features acquired at the beginning of the response curve of the sensors. So, in this study only transient features are studied for discrimination of six different gases in the presence of long-term drift. A typical response of 16 sensors array (having four different type of gas sensors) towards a particular gas (Ethanol) can be seen in Fig. 1. Upon the exposure of gas to sensors, the resistance of gas sensors starts to increase, the initial stage of response from where the response starts increasing from its baseline until it reaches a steady state is called its initial transient state. The region when the response reaches its maximum value and remains almost linear is the steady state region and the region when the response starts going back to its baseline value is the final transient state region. All these three regions are marked in Fig. 2. The features extracted from the initial transient state are of interest in this study, because if only initial transient features are used, the system does not need to wait for the steady state and final transient features. Thus, decreasing the response time of the system.

The initial transient features used in this study are calculated by the authors of [30], using the exponential moving average function as:

$$Y_\alpha[k] = (1-\alpha)\, Y_\alpha[k-1] + \alpha\,(r[k] - r[k-1]) \tag{1}$$

where, $r[k]$ represents the sensor's time series response at time k and α is a smoothing factor. Using three different values of α in (1), three different features for each gas sensor TF_{sensor_i} are computed from the rising portion of the response curve as:

$$TF_{sensor_i} = \begin{cases} \max\limits_k ema_{\alpha=0.001}(r[k]) \\ \max\limits_k ema_{\alpha=0.01}(r[k]) \\ \max\limits_k ema_{\alpha=0.1}(r[k]) \end{cases} \tag{2}$$

The sensors array used in this study contains 16 gas sensors and for each gas sensor three initial transient features are extracted, thus creating a feature vector of size 48. Four different types of sensors are used for acquisition of the data which are TGS2600, TGS2602, TGS2610 and TGS2620 (4 each). These sensors are manufactured and tagged by Figaro Inc. The response of these gas sensors is a sixteen channel time series response which represents the change in resistance on the active layer of the sensors. A test chamber of 60 ml volume is used to expose the sensors array to different VOCs individually with different concentration values. The concentrations are controlled with three mass flow controllers (MFCs) and the exposure is done in a random manner. The flow rate is set to 200 ml/min and the sampling rate used is 100 Hz. Based on the time of acquisition, the data is placed in ten different batches. A complete description of the hardware setup is given in [30].

B. Sample Cleaning/Denoising

The sample cleaning/denoising is performed to mitigate the effect of overall sensors drift and noise in data. In order to do the sample cleaning, a modified distance based boxplot approach is used. The data sample/observation under consideration is evaluated for possible outliers or noisy data points that may occur due to the sensors drift. If any element in an observation deviates significantly from the other element/entries in the same observation then it is detected as a noisy/drifted data element and it is replaced by the mean of non-drifted entries of the same observation.

Rather than using the traditional boxplot to identify the outliers from the unique dimensions, one useful idea is to calculate the distance between all the data points and to use the resulting distance vector for identifying the outliers. The use of distance vector enhances the ability of boxplot by considering the compactness of data. Consider the case of a data sample $S_n \in \mathbb{R}$, the n dimensional data sample can be transformed to a distance vector d_n, by computing the distance of each observation in S to its k^{th} closest neighbor. The concept of transformation can be summarized as the following function:

$$S_n \xrightarrow{k} d_n \tag{3}$$

where, $d_n \in \mathbb{R}$ is a vector of length n containing the Euclidian distance of each observation in S to its k^{th} closest neighbor and d_n can be further used to compute a modified boxplot

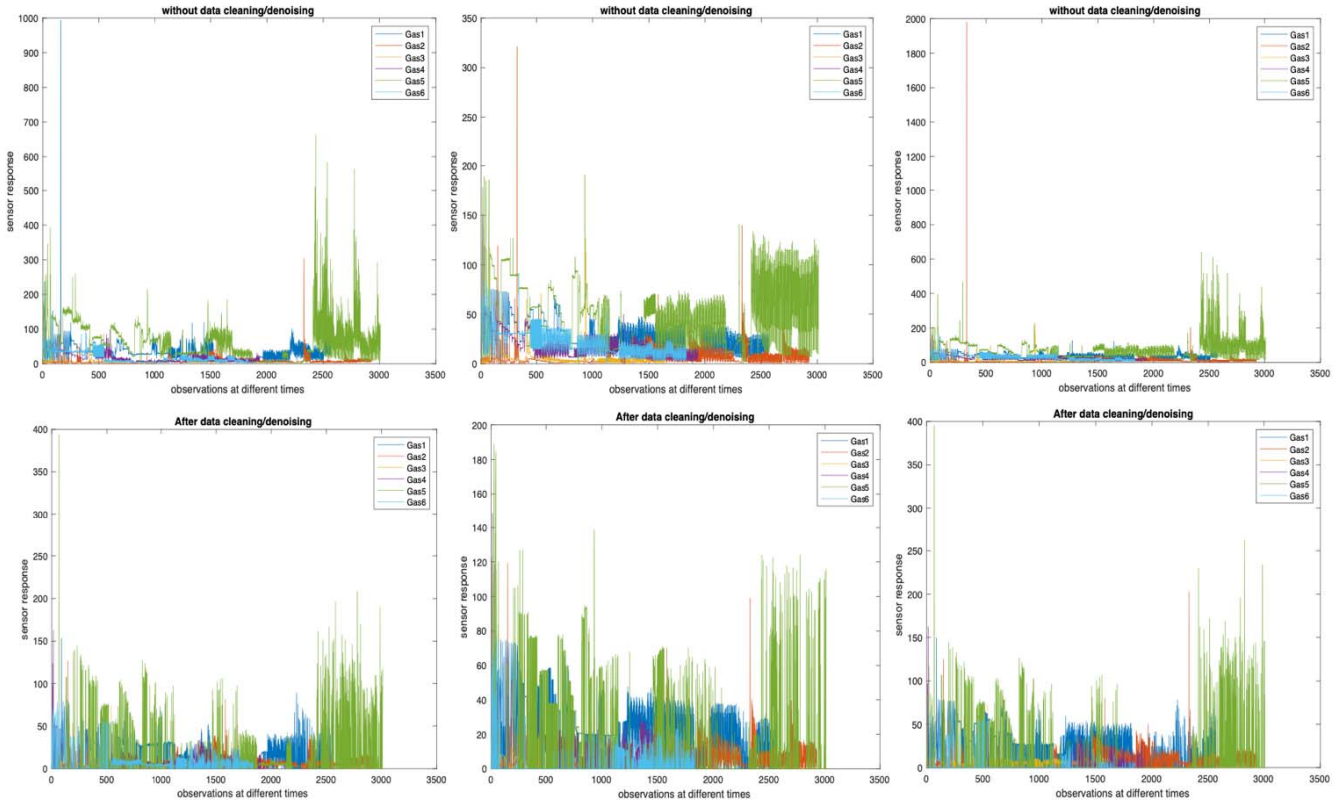

Fig. 3. Data cleaning/denoising. Row 1: response of three sensors to six different gases without denoising. Row 2: response of sensors after denoising.

with extreme values are computed as:

$$\begin{cases} LE_{d_n} = Q1_{d_n} - c_1\left(Q2_{d_n} - Q1_{d_n}\right), \\ UE_{d_n} = Q3_{d_n} + c_2\left(Q3_{d_n} - Q2_{d_n}\right). \end{cases} \tag{4}$$

where, LE_{d_n} and UE_{d_n} are respectively the lower and upper extreme values of the modified boxplot and $Q1_{d_n}$, $Q2_{d_n}$, and $Q3_{d_n}$ are the first, second and third quartiles of the boxplot.

The outliers can be identified as the observations that lie outside the defined extreme values in (4). The constants c_1 and c_2 can either be tuned for better performance or can be kept constant as equal to 1.5 or 3 as suggested by different authors in the literature. The resulting box-whisker plot is easy to implement and can identify the underlying outliers in a dataset accurately. For-example, in Fig. 3 the modified boxplot technique is applied on three different sensors against their response to six different gases. From the results it can be seen that, denoising the samples removes majority of the peaks present in the raw features and gives more stability to the response behavior. Here, in this paper the values of $k = 3$ and $c_1 = c_2 = 3$ are kept fixed for all the experimentation and the detected outliers are replaced by the sample inlier mean values.

C. Features Optimization

Optimization of sensors array in an ENS is required to find out the best combination of sensors for a particular application. Furthermore, feature selection algorithms reduce the dimensionality of the data and contribute towards memory requirement, power consumption, computational overhead and production cost [31]. Besides these advantages, feature selection can also mitigate the effect of sensors drift [27]. In order to further investigate the ability of feature selection to mitigate the effect of drift, this study uses only transient features to classify six different gases collected using the same sensors array over a period of 36 months [30].

Wrapper feature selection methods are considered more suitable as compared to the filter selection methods due to their interaction with the classifier. As the filter based methods are independent of the classifier their accuracy is always expected to be low as compared to the wrapper methods. However, wrapper based methods are prone to overfitting and require a thorough validation.

Metaheuristics feature selection algorithms like Particle Swarm Optimization (PSO) and Shuffled Frog-Leaping (SFL) in a wrapper setup are found suitable for optimizing the sensors array for an ENS [32]–[34]. In this study, the ability of PSO is further enhanced by a modified boxplot to cope with sensors drift and multiple classifiers in a tree setup are wrapped with PSO for classification of gases.

The problem of sensors array optimization using PSO is a discrete optimization problem which is solved by the following three basic steps:

Step 1: Computing the fitness of particles against an objective function.

Step 2: Updating the personal and global best fitness and positions of particles.

Step 3: Updating the velocities and positions of particles in the swarm.

These steps are iterated until a stopping criteria is reached.

The velocities and positions of the swarm are initialized randomly as:

$$V = \begin{bmatrix} v_{11} & v_{12} & \dots & v_{1n} \\ v_{21} & v_{22} & \dots & v_{2n} \\ \vdots & \vdots & \vdots & \vdots \\ v_{m1} & v_{m2} & \dots & v_{mn} \end{bmatrix}_{m \times n} \tag{5}$$

$$v_{ij} = -v_{max} + 2v_{max} \times rand() \tag{6}$$

$$X = \begin{bmatrix} x_{11} & x_{12} & \dots & x_{1n} \\ x_{21} & x_{22} & \dots & x_{2n} \\ \vdots & \vdots & \vdots & \vdots \\ x_{m1} & x_{m2} & \dots & x_{mn} \end{bmatrix}_{m \times n} \tag{7}$$

$$x_{ij} = randint() \tag{8}$$

where, v_{max} is the maximum velocity with which a particle can accelerate and it is a user specified value to control exploration, $randint()$ is a function that generates a random binary matrix for defining the initial positions of particles, m represents the swarm size and n is the size of each particle (is equal to the length of feature vector).

Once a swarm of particles is initialized, PSO evaluates each particle in the swarm against a fitness function. Here, each particle's position is a combination of binary bits which indicates either selection of feature (if the index location is 1) or non-selection of feature (if the index location is 0). The features with index location 1 are evaluated for classification and the classification error is returned as a fitness value of the model. The fitness function is defined as:

$$F_i = CE\left(x_{i1}, x_{i2}, \dots, x_{in}\right); \quad \forall x_{ij} == 1 \tag{9}$$

where, F_i is the fitness of i^{th} particle, CE is the classification error after evaluating the combination of features $(x_{i1}, x_{i2}, \dots, x_{in})$ with index location x_{ij} equal to 1 and n is the length of feature vector. Global best particle is the one with lowest F_i.

After evaluating all the particles in swarm against a fitness function, the velocities and positions of the particles are updated for re-evaluation in the next iteration. The velocity of particles is updated as:

$$v_i(t+1) = w \times v(t) + c_1 \times r_1 \times [p(t) - x_i(t)] + c_2 \times r_2 \times [g(t) - x_i(t)] \tag{10}$$

where, i represents the i^{th} particle whose velocity is being updated, $v_i(t)$ is the velocity of i^{th} particle at iteration t, $x_i(t)$ is the position of i^{th} particle at iteration t, w is the inertia constant, c_1 $(0 \leq c_1 \leq 2)$ and c_2 $(0 \leq c_2 \leq 2)$ are exploration and exploitation constants, $g(t)$ is the global best position of the swarm at iteration t and $p(t)$ is the personal best position of the i^{th} particle at iteration t.

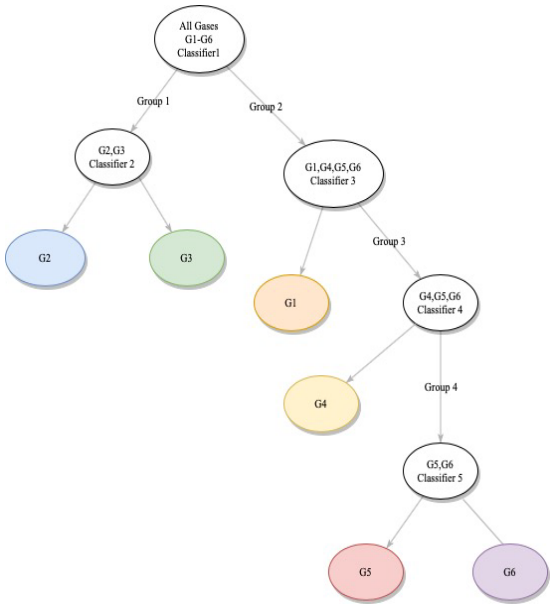

Fig. 4. Classification model for drift compensation.

The position $X_i\left(x_{i1}, x_{i2}, \dots, x_{in}\right)$ of the i^{th} particle is updated as:

$$if rand() < S\left(v_{ij}(t)\right) \tag{11}$$
$$x_{ij} = 1$$
$$else,$$
$$x_{ij} = 0.$$

$$S\left(v_{ij}(t)\right) = \frac{1}{1 + e^{-\left(v_{ij}(t)\right)}} \tag{12}$$

where, $rand()$ is a uniformly distributed $U(0, 1)$ random number and $S(.)$ is the sigmoid function. After each iteration the personal best and global best positions and fitness are updated by comparing the fitness values to the previously achieved fitness values. Once the algorithm completes the maximum allowed number of iterations the best combination of features for classification can be found in the global best position of the swarm.

D. Classification Setup

The problem of multi-class classification in the presence of long-term sensors drift is solved by using the strategy of dividing the main problem into sub-problems. At the initial stage of classification, only those optimum features are searched which can classify all the six gases in two sub-groups using classifier number 1. Group 1 contains Gas2 and Gas3 while Group2 has Gas1, Gas4, Gas5 and Gas6. In the second stage of classification Gas2 and Gas3 are further classified using classifier number 2 with its own optimized features and the gases in Group2 are further classified as Gas1 and Group3. In the third stage of classification the gases in Group3 are further classified as Gas4 and Group4 using classifier number 4, with different optimized subset of features. In the last stage of classification, the gases in Group4 are classified as Gas5 and Gas6 using classifier number 5. The overall structure of the classification model is described in Fig. 4. This specific classification setup

TABLE I
TRANSIENT FEATURES USED FOR EXPERIMENTATION

	S1	S2	S3	S4	S5	S6	S7	S8	S9	S10	S11	S12	S13	S14	S15	S16
$\alpha = 0.001$	F1	F4	F7	F10	F13	F16	F19	F22	F25	F28	F31	F34	F37	F40	F43	F46
$\alpha = 0.01$	F2	F5	F8	F11	F14	F17	F20	F23	F26	F29	F32	F35	F38	F41	F44	F47
$\alpha = 0.1$	F3	F6	F9	F12	F15	F18	F21	F24	F27	F30	F33	F36	F39	F42	F45	F48

is adapted after a comprehensive experimentation on grouping and identification of the VOCs under consideration which is further elaborated for better understanding in the performance evaluation section.

In the proposed tree structured classification model, each node contains a different classifier optimized with different subset of transient features. The classifier at each node is selected after a thorough experimentation of different classification models and the selection is based on the best performing model for the gases of interest. Each node uses its own separately optimized subset of transient features to enhance the overall classification performance of the system. The classifiers tested at each node include Support Vector Machines (SVM), K-Nearest Neighbor (KNN), Naïve Bayes (NB), Discriminant Analysis (DA), Logistic Regression (LR) and Decision Tree (DT).

IV. PERFORMANCE EVALUATION

The proposed drift compensation model based on the initial transient features of the response curve is tested using a famous large scale benchmark drift dataset freely available online at UCI Machine Learning repository. A brief description of the dataset and the performance of the proposed model follows in this section.

A. Dataset

The dataset used in this study for performance evaluation was acquired using an array of 16 gas sensors manufactured by Figaro Inc. The sensors used in the array are TGS2600, TGS2602, TGS2610 and TGS2620. Six different analytes are used in the collection of dataset over a period of 36 months using the same sensors array. The analytes used are Ammonia, Ethanol, Acetone, Acetaldehyde, Toluene and Ethylene. A wide range of concentration variation (between 5-1000 ppmv) is exposed to the sensors array to test the ability of sensors sensitivity against low and high concentration of these pure gaseous substances. A total of 13910 measurements are recorded and based on the time of acquisition these measurements are organized in 10 different batches. For-example the measurements recorded in first two months are placed in batch1 and the measurements recorded in the last 36^{th} month are placed in batch10. As the data is organized in different batches based on the time of acquisition, the effect of long term drift gradually increases with an increase in batch number. In order to demonstrate the effect of drift on the distribution of data, measurements recorded for Ethylene using a fixed concentration level (100 ppmv) are shown in Fig. 5. It can be observed from the distribution of data in Fig. 5 that if a ML model is trained on data contained in Batch 1, it will fail to correctly predict the data in Batches 2-10 as the distribution

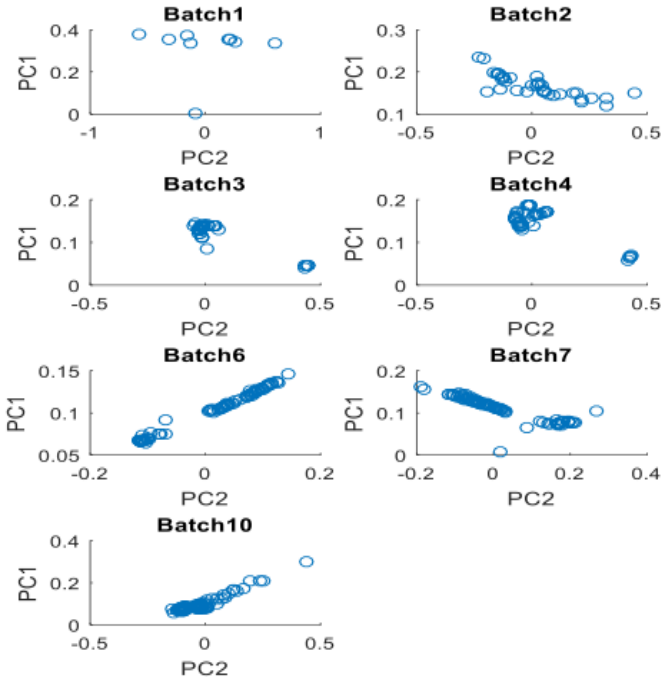

Fig. 5. Effect of drift on distribution of data for Ethylene with a fixed level of concentration (100 ppmv), y-axis and x-axis are the first and second Principal Component (PC) of the feature vector.

is totally random in upcoming batches due to drift. Therefore, a strategy to compensate the drift has to be incorporated in a ML model.

In the actual dataset provided by the authors of [30], the features extracted are both the transient features and the steady state features. For each of the 16 gas sensors, 2 steady state and 6 transient features are computed, making a feature vector of 128 in length. Among the six transient features 3 features against each sensor are computed from the initial rising state of the time series response curve and 3 are computed from the final decaying portion of the response curve.

The aim of this study is to use only the initial transient features, so the features extracted only during the initial rising response curve of the sensors are used. Thus, only 3 features against each gas sensor are used and this makes a feature vector of length 48 (16 sensors x 3 features). The feature vector is explained using Table I, where each feature number (F1-F48) can be mapped to its correspondence sensor number (S1-S16) and the value of smoothing factor α used for computing the respective feature value in (1)-(2).

B. Results

The details of dataset used are reported in Table II. For evaluation of proposed drift compensation model, the data contained in batch1 is used as training data for classifier

TABLE II
DETAILS OF DATASET – CONCENTRATIONS OF ANALYTES – TRAINING DATA SAMPLES – TESTING DATA SAMPLES AND – TOTAL DATA SAMPLES

Gas	Concentrations (ppmv)	Training	Testing									
		Batch1	Batch2	Batch3	Batch4	Batch5	Batch6	Batch7	Batch8	Batch9	Batch10	**All**
Ammonia	2.5-1000	83	100	216	12	20	110	360	40	100	600	1641
Ethanol	2.5-600	90	164	365	64	28	514	649	30	61	600	2565
Ethylene	2.5-300	98	334	490	43	40	574	662	30	55	600	2926
Acetaldehyde	2.5-300	30	109	240	30	46	29	744	33	75	600	1936
Acetone	10-1000	70	532	275	12	63	606	630	143	78	600	3009
Toluene	1-230	74	5	0	0	0	467	568	18	101	600	1833
Total		**445**	**1244**	**1586**	**161**	**197**	**2300**	**3613**	**294**	**470**	**3600**	**13910**

TABLE III
CLASSIFICATION PERFORMANCE OF STATE-OF-ART CLASSIFIERS USING ALL RAW TRANSIENT FEATURES

Classifier	Type	Accuracy	Sensitivity	Specificity
SVM	Gaussian	0.1223	0.1720	0.8345
	Polynomial Degree 2	0.3271	0.3209	0.8654
	Polynomial Degree 3	0.3274	0.3135	0.8630
	Linear	0.4105	0.4111	0.8801
KNN	K=1	0.2938	0.2558	0.8568
	K=3	0.3143	0.2722	0.8619
	K=5	0.3131	0.2659	0.8611
	K=7	0.3032	0.2563	0.8592
DA	linear	0.1593	0.1949	0.8378
	pseudolinear	0.1593	0.1949	0.8378
	pseudo-quadratic	0.2591	0.3003	0.8585
LR	linear	0.3646	0.3242	0.8707
NB	multiclass	0.2785	0.2371	0.8554
DT	multiclass	0.3293	0.3182	0.8673

TABLE IV
CLASSIFICATION PERFORMANCE OF STATE-OF-ART CLASSIFIERS USING ALL THE TRANSIENT FEATURES AFTER DATA CLEANING

Classifier	Type	Accuracy	Sensitivity	Specificity
SVM	Gaussian	0.1421	0.1787	0.8355
	Polynomial Degree 2	0.2545	0.2564	0.8528
	Polynomial Degree 3	0.4173	0.4111	0.8817
	Linear	0.4160	0.4079	0.8805
KNN	K=1	0.3446	0.3488	0.8679
	K=3	0.3488	0.3549	0.8717
	K=5	0.3418	0.3471	0.8706
	K=7	0.3444	0.3495	0.8710
DA	linear	0.2626	0.2876	0.8533
	pseudolinear	0.2626	0.2876	0.8533
	pseudo-quadratic	0.2717	0.3018	0.8604
LR	linear	0.3914	0.3665	0.8762
NB	multiclass	0.2965	0.2650	0.8599
DT	multiclass	0.3455	0.3368	0.8684

TABLE V
CLASSIFICATION PERFORMANCE OF STATE-OF-ART CLASSIFIERS AFTER DATA CLEANING AND FEATURE SELECTION

Classifier	Selected Features	Accuracy
SVM (linear kernel)	4,8,10,18,19,40,41	0.6522
KNN (Cosine, K=1)	16,32,37,40,41,46	0.5934
DA (linear)	4,6,12,25,27,32,34,39,40,41	0.6816
LR (linear)	2,4,10,15,32,34,41	0.6479
NB	4,7,17,19,24,25,31,40,41,44,45,48	0.4793
DT (AdaBoostM2)	6,10,15,16,28,31,39	0.5144

TABLE VI
DA CONFUSION MATRIX

Total 13465		**Predicted Class**					
		Gas1	Gas2	Gas3	Gas4	Gas5	Gas6
Actual Class	Gas 1	1815	31	109	127	16	377
	Gas 2	31	2632	105	3	51	6
	Gas 3	52	20	1331	8	113	34
	Gas 4	684	45	4	262	207	704
	Gas 5	193	121	164	458	1760	243
	Gas 6	83	51	27	88	132	1378

TABLE VII
DA PERFORMANCE EVALUATION PARAMETERS

Accuracy	0.6816
Sensitivity	0.6730
Specificity	0.9368
Error	0.3184
Precision	0.6432
F1_score	0.6462
False Positive Rate	0.0632
Kappa	0.1275
Matthews Correlation Coefficient	0.5923

learning and the data contained in batches 2-10 is used as the testing data. This is done primarily to evaluate the performance of the proposed ML model against drift by training it on almost drift free data (batch1) and testing it on the drifted data (batch 2-10). The data in batch1 is considered drift free because this data was acquired when the sensors were new. The results of different state-of-the-art classifiers for classification of all six gases using all the 48 initial transient features are given in Table III. Here, the features are used in their original form without doing any processing to compensate the drift. It can be seen from the results in Table III that if these transient features are used in their actual form, none of the classifier is able to discriminate between gases in the presence of drift. The maximum accuracy achieved is 41.05% using the linear SVM which shows that the classical ML algorithms fail to perform when trained on almost drift free data and tested on the drifted data.

The same transient features are processed using the modified boxplot technique described in section III-B and the noisy data points contained within a sample are replaced by the mean of inlier data samples. After performing the proposed data cleaning process, the same state-of-the-art classifiers are evaluated again and the results are reported in Table IV. It can be seen from the results in Table IV that the data cleaning process has contributed towards an increase in the classification accuracy

TABLE VIII
BEST CLASSIFICATION RESULTS AT EACH NODE OF THE PROPOSED MULTI-CLASSIFIER TREE APPROACH

Node	Classification	Best Classifier	Features	Accuracy
1	Group1, Group2	KNN (Cosine Distance, K=7)	7,10,11,20,26,29,31,32,35,38,42,47	0.9806
2	Gas2, Gas3	LDA	22,29,36,39,40	0.9744
3	Gas1, Group3	SVM (linear)	7,15,16,32,34	0.9111
4	Gas4, Group4	SVM (linear)	9,11,17,21,23,28,32,33,35,37,43	0.8750
5	Gas5, Gas6	SVM (linear)	3,5,10,22,35,40,48	0.9636

of all the classifiers. However, the overall accuracy to classify the gases in presence of drift remains low.

To further enhance the classification performance of classifiers, feature selection process is carried out using PSO as described in section III-C. The best classification results after feature selection and optimization of hyperparameters of all the classifiers are given in Table V.

The results reported in Table V give a clear insight that feature selection has the ability to compensate sensors drift and when combined with a data cleaning preprocessing step the best classification accuracy has increased from 41.05% to 68.16%. To further get more clear insight of the classification performance of the best performing classifier (DA), confusion matrix and some other performance evaluation parameters are computed and the results are given in Table VI and Table VII, respectively.

From the results in Table VI, it can be observed that although the classifier has ability to discriminate some gases but there exists an overlap between some gases which contributes to the misclassifications. For-example a clear overlap between Gas1, Gas4, Gas5 and Gas6 is observed, as majority of Gas4 and Gas5 samples are either misclassified as Gas1 or Gas6. Based on this observation, the Gases are classified by dividing the overall multiclass classification problem into subproblems. For example, at the initial classification stage the gases are only classified as Group1 (Gas2 and Gas3) and Group2 (Gas1, Gas4, Gas5, and Gas6). In further classification stages these Groups are either classified as recognized gases or new groups as previously described in the proposed classification architecture (Fig. 4). In order to maximize the classification ability of the proposed multi-classifier tree approach, all the nodes of the tree structured classifier are optimized separately in terms of the classifier used and the selected features. The best classification results after evaluating each of the state-of-art classifier, at each node of the proposed multi-classifier tree approach, are given in Table VIII.

The overall performance of the proposed multi-classifier tree approach for discriminating all the six gases in the presence of long-term sensors drift is reported using a confusion matrix and performance evaluation parameters in Table IX and Table X, respectively. The proposed classification approach using only transient features, combined with a data cleaning preprocessing step and feature optimization resulted in an overall accuracy of 87.34%, with 87.23% sensitivity and 97.47% specificity. The performance of proposed architecture with respect to individual gases is reported in Table XI.

TABLE IX
CONFUSION MATRIX FOR PROPOSED MULTI-CLASSIFIER TREE APPROACH

Total 13465		**Predicted Class**					
		Gas1	Gas2	Gas3	Gas4	Gas5	Gas6
Actual Class	Gas 1	1952	0	0	523	0	0
	Gas 2	74	2679	75	0	0	0
	Gas 3	35	18	1505	0	0	0
	Gas 4	0	0	0	1469	400	37
	Gas 5	0	0	0	226	2634	79
	Gas 6	0	0	0	162	76	1521

TABLE X
DA PERFORMANCE EVALUATION PARAMETERS

Accuracy	0.8734
Sensitivity	0.8723
Specificity	0.9747
Error	0.1266
Precision	0.8810
F1_score	0.8736
False Positive Rate	0.0253
Kappa	0.5442
Matthews Correlation Coefficient	0.8503

TABLE XI
PERFORMANCE OF PROPOSED MULTI-CLASSIFIER TREE FOR INDIVIDUAL GASES

Gas	Name	Accuracy	Sensitivity	Specificity	F1score
1	Ethanol	0.9530	0.7886	0.9900	0.8606
2	Ethylene	0.9875	0.9473	0.9983	0.9697
3	Ammonia	0.9904	0.9659	0.9937	0.9592
4	Acetaldehyde	0.8998	0.7707	0.9211	0.6854
5	Acetone	0.9419	0.8962	0.9547	0.8708
6	Toluene	0.9737	0.8647	0.9900	0.8957

C. Comparison With State-of-Art Approaches

The proposed approach (using only transient features) for a faster system response is compared with the existing state-of-art approaches in terms of classification accuracy and the results are reported in Table XII. The results for Kernel PCA (KPCA), Geodesic Flow Kernel (GFK), marginalized Stacked Denoising Autoencoder (mSDA), Information- Theoretical Learning (ITL), Structural Correspondence Learning (SCL), Subspace Alignment (SA), Transfer Component Analysis (TCA), Maximum Independence Domain Adaptation (MIDA), Semi-supervised MIDA (SMIDA) and Semi-Supervised TCA (SSTCA), are taken from [35]. The results for multi class SVM with Radial Basis Function (RBF) kernel, Component Correction PCA (CC-PCA), Extreme Learning Machine (ELM) with RBF kernel (ELM-rbf), Geodesic Flow Kernel (GFK), Combination kernel (comgfk), Domain Adaptation ELM (DAELM-S and DAELM-T) are taken from [36]. The results for Multi-Feature Kernel Semi-Supervised joint

TABLE XII
COMPARISON WITH EXISTING STATE-OF-THE-ART APPROACHES

Batch/Testing Samples	**2**/1244	**3**/1586	**4**/161	**5**/197	**6**/2300	**7**/3613	**8**/294	**9**/470	**10**/3600	**All**/13465	Features	Reference
KPCA	75.88	69.04	49.07	57.87	62.65	52.26	37.07	47.66	49.97	57.13		
GFK	77.41	80.26	71.43	76.14	77.65	64.99	36.39	47.45	48.72	64.75		
mSDA	73.87	79.19	65.84	80.20	76.39	65.90	51.70	48.51	48.92	64.75		
ITL	76.85	79.45	59.63	96.45	78.00	60.95	49.32	77.02	48.58	65.01		
SCL	77.57	82.03	68.32	82.74	77.22	65.18	53.74	48.51	48.08	65.26		
SA	80.79	80.01	71.43	75.63	78.35	64.68	52.04	48.51	48.08	65.26	**Transient**	[35]
SMIDA (discrete)	80.47	87.07	65.22	75.63	87.61	62.44	48.30	67.87	48.36	67.47	+ Steady	
TCA	82.96	81.97	65.22	76.14	89.09	58.98	49.32	66.17	49.50	66.88	state	
MIDA (discrete)	81.03	85.62	60.25	75.63	87.61	62.44	48.30	67.87	48.36	67.47		
MIDA (continuous)	84.32	81.59	68.32	75.63	91.74	63.13	78.91	62.34	45.14	67.90		
SMIDA (no aug.)	82.23	83.17	67.70	75.13	85.22	61.67	51.02	61.49	54.61	68.27		
SMIDA	83.68	82.28	73.91	75.63	93.00	63.49	79.25	62.34	45.50	68.41		
SSTCA	84.57	80.90	80.12	75.63	87.26	66.37	54.76	61.28	54.44	70.01		
SVM (rbf)	74.36	61.03	50.93	18.27	28.26	28.81	20.07	34.26	34.47	38.34		
CC-PCA	67.00	48.50	41.00	35.50	55.00	31.00	56.50	46.50	30.50	41.64		
ML-rbf	42.25	73.69	75.53	66.75	77.51	54.43	33.50	23.57	34.92	53.20		
ELM-rbf	70.63	66.44	66.83	63.45	69.73	51.23	49.76	49.83	33.50	53.52		
SVM (gfk)	72.75	70.08	60.75	75.08	73.82	54.53	55.44	69.62	41.78	58.85		
SVM (comgfk)	74.47	70.15	59.78	75.09	73.99	54.59	55.88	70.23	41.85	59.10	**Transient**	[36]
ML- comgfk	80.25	74.99	78.79	67.41	77.82	71.68	49.96	50.79	53.79	67.95	+ Steady	
DAELM-S (20)	87.57	96.53	82.61	81.47	84.97	71.89	78.10	87.02	57.42	75.54	state	
DAELM-T (40)	83.52	96.34	88.20	99.49	78.43	80.93	87.42	100.00	56.25	77.12		
DAELM-S (30)	87.98	95.74	85.16	95.99	94.14	83.51	86.90	100.00	53.62	80.04		
DAELM-T (50)	97.96	95.34	99.32	99.24	97.03	83.09	95.27	100.00	59.45	83.25		
MFKS (10)	80.79	80.64	86.75	79.14	80.69	36.19	68.30	63.04	37.10	56.26	**Transient**	[37]
MFKS (20)	85.45	77.96	88.65	83.61	89.38	68.80	84.67	78.66	42.54	69.06	+ Steady	
											state	
Multi-classifier Tree	90.03	99.17	87.58	65.48	94.91	89.37	86.73	71.91	78.00	**87.34**	**Transient**	**Proposed**

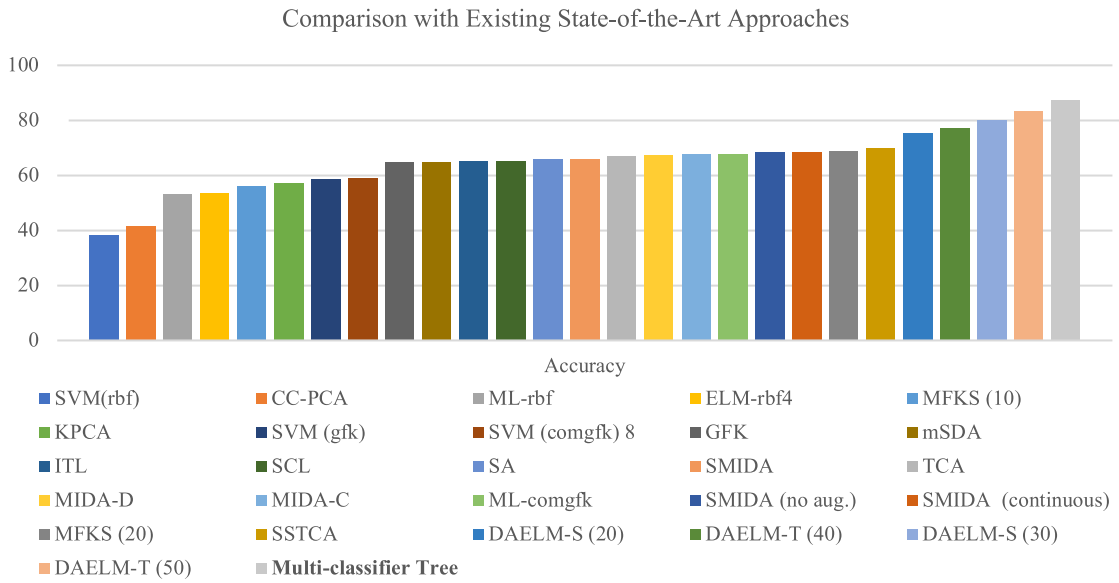

Fig. 6. Comparison in terms of overall classification accuracy (All Data).

learning (MFKS) are taken from [37]. A visual comparison in terms of classification performance is provided in Fig. 6.

It can be observed from the results in Table XII that the proposed Multi-Classifier tree approach has shown better performance to compensate the sensors drift, using only transient features. As the proposed model depends only on the initial transient response of sensors, the overall system response decreases making the system faster as compared to the existing approaches. For example, from the response of a typical gas sensor shown in Fig. 2, it can be seen that a model that depends on entire sensor response has to wait almost 600-700 seconds before starting the process of recognition, whereas the proposed model only has to wait 100-200 seconds to start the recognition process. This shows that besides performing better in terms of classification accuracy the proposed approach is also better in terms of time complexity. Furthermore, keeping in view the performance of the proposed model against drift when trained only on the data acquired in the initial two months (when the sensors are new), it is expected that if any of the sensor in the sensor's

array needs a replacement, it can be done without requiring any retraining of the model if new sensor of the same type is available. However, if a new sensor of the same type is not available due to any reason and the replacement needs to be done with a different type of sensor or a relatively old sensor of same type, the model will require retraining to ensure the best classification performance.

The important conclusions drawn from this study are as follows: (i) Feature selection plays a vital role in drift compensation of gas sensors. (ii) Initial Transient response of Figaro Gas sensors (TGS2600, TGS2602, TGS2610 and TGS2620) have an ability to discriminate between different analytes in the presence of drift. (iii) Figaro gas sensors when combined with a powerful classification algorithm are highly sensitive towards Ethylene and Ammonia, even in the presence of long term drift.

V. Conclusion

In this study, two challenging problems: (i) sensors long term drift and (ii) system's large latency are simultaneously solved using a powerful ML model optimized with a combination of initial transient features. The proposed approach is based entirely on ML techniques and therefore it does not require any system recalibration or sensors replacement. Furthermore, contrary to the ML solutions available in existing literature the proposed solution does not depend on any target domain data for classifier learning and is based only on the source domain data for learning.

The proposed model is trained and tested on drifted transition data that was acquired over a period of 36 months and the proposed model is found robust against drift with an overall classification accuracy of 87.34%. A multi-classifier tree approach is proposed to handle long term sensors drift and for reduced system's response time initial transient response of sensors is used as features for learning the classifier. Furthermore, the study shows the importance of feature selection in compensating drift for gas sensors and it is seen that a suitable combination of initial transient features has powerful discriminatory abilities in the presence of long-term sensors drift. The merits of the proposed approach include its ability to perform in the presence of long-term drift and its dependence only on the initial transient features for a faster system response. This makes the proposed approach feasible for real time critical applications of an ENS.

Acknowledgment

The publication of this article was funded by the Qatar National Library. The authors would like to acknowledge the library for supporting the publication of this article.

References

[1] H. Cao, P. Jia, D. Xu, Y. Jiang, and S. Qiao, "Feature extraction of citrus juice during storage for electronic nose based on cellular neural network," *IEEE Sensors J.*, vol. 20, no. 7, pp. 3803–3812, Apr. 2020.

[2] Y. Yang, H. Liu, and Y. Gu, "A model transfer learning framework with back-propagation neural network for wine and chinese liquor detection by electronic nose," *IEEE Access*, vol. 8, pp. 105278–105285, 2020.

[3] G. Zambotti *et al.*, "Early detection of fish degradation by electronic nose," in *Proc. IEEE Int. Symp. Olfaction Electron. Nose (ISOEN)*, May 2019, pp. 1–3.

[4] H. Sun *et al.*, "Sensor array optimization of electronic nose for detection of bacteria in wound infection," *IEEE Trans. Ind. Electron.*, vol. 64, no. 9, pp. 7350–7358, Sep. 2017.

[5] O. Zaim, T. Saidi, N. El Bari, and B. Bouchikhi, "Assessment of 'breath print' in patients with chronic kidney disease during dialysis by non-invasive breath screening of exhaled volatile compounds using an electronic nose," in *Proc. IEEE Int. Symp. Olfaction Electron. Nose (ISOEN)*, May 2019, pp. 1–4.

[6] A. Gongora, A. Jaenal, D. Chaves, J. Monroy, and J. Gonzalez-Jimenez, "Urban monitoring of unpleasant odors with a handheld electronic nose," in *Proc. IEEE Int. Symp. Olfaction Electron. Nose (ISOEN)*, May 2019, pp. 1–3.

[7] L. Capelli and S. Sironi, "Monitoring odour emisssions from an oil & gas plant: Electronic nose performance testing in the field," in *Proc. ISOCS/IEEE Int. Symp. Olfaction Electron. Nose (ISOEN)*, May 2017, pp. 1–3.

[8] M. Adib, R. Eckstein, G. Hernandez-Sosa, M. Sommer, and U. Lemmer, "SnO_2 nanowire-based aerosol jet printed electronic nose as fire detector," *IEEE Sensors J.*, vol. 18, no. 2, pp. 494–500, Jan. 2018.

[9] V. S. P. Rao *et al.*, "E-Nose: Multichannel analog signal conditioning circuit with pattern recognition for explosive sensing," *IEEE Sensors J.*, vol. 20, no. 3, pp. 1373–1382, Feb. 2020.

[10] S. Di and M. Falasconi, "Drift correction methods for gas chemical sensors in artificial olfaction systems: Techniques and challenges," in *Advanced Chemical Sensors*. Rijeka, Croatia: InTech, Jan. 2012, pp. 305–326.

[11] M. Holmberg, F. A. M. Davide, C. Di Natale, A. D'Amico, F. Winquist, and I. Lundström, "Drift counteraction in odour recognition applications: Lifelong calibration method," *Sens. Actuators B, Chem.*, vol. 42, no. 3, pp. 185–194, Aug. 1997.

[12] E. Llobet, J. Brezmes, X. Vilanova, J. E. Sueiras, and X. Correig, "Qualitative and quantitative analysis of volatile organic compounds using transient and steady-state responses of a thick-film tin oxide gas sensor array," *Sens. Actuators B, Chem.*, vol. 41, nos. 1–3, pp. 13–21, Jun. 1997.

[13] A. C. Romain and J. Nicolas, "Long term stability of metal oxide-based gas sensors for e-nose environmental applications: An overview," *Sens. Actuators B, Chem.*, vol. 146, no. 2, pp. 502–506, Apr. 2010.

[14] A.-C. Romain, P. André, and J. Nicolas, "Three years experiment with the same tin oxide sensor arrays for the identification of malodorous sources in the environment," *Sens. Actuators B, Chem.*, vol. 84, nos. 2–3, pp. 271–277, May 2002.

[15] S. Feng *et al.*, "Review on smart gas sensing technology," *Sensors*, vol. 19, no. 17, p. 3760, Aug. 2019.

[16] Q. Liu, X. Li, M. Ye, S. S. Ge, and X. Du, "Drift compensation for electronic nose by semi-supervised domain adaption," *IEEE Sensors J.*, vol. 14, no. 3, pp. 657–665, Mar. 2014.

[17] S. Marco and A. Gutierrez-Galvez, "Signal and data processing for machine olfaction and chemical sensing: A review," *IEEE Sensors J.*, vol. 12, no. 11, pp. 3189–3214, Nov. 2012.

[18] L. Carmel, S. Levy, D. Lancet, and D. Harel, "A feature extraction method for chemical sensors in electronic noses," *Sens. Actuators B, Chem.*, vol. 93, nos. 1–3, pp. 67–76, Aug. 2003.

[19] C. Distante, M. Leo, P. Siciliano, and K. C. Persaud, "On the study of feature extraction methods for an electronic nose," *Sens. Actuators B, Chem.*, vol. 87, no. 2, pp. 274–288, Dec. 2002.

[20] C. Distante, P. Sicilian, and K. C. Persaud, "Dynamic cluster recognition with multiple self-organising maps," *Pattern Anal. Appl.*, vol. 5, no. 3, pp. 306–315, Aug. 2002.

[21] T. Artursson, T. Eklöv, I. Lundström, P. Mårtensson, M. Sjöström, and M. Holmberg, "Drift correction for gas sensors using multivariate methods," *J. Chemometrics*, vol. 14, nos. 5–6, pp. 711–723, 2000.

[22] T. Liu, Y. Chen, D. Li, T. Yang, J. Cao, and M. Wu, "Drift compensation for an electronic nose by adaptive subspace learning," *IEEE Sensors J.*, vol. 20, no. 1, pp. 337–347, Jan. 2020.

[23] L. Zhang, Y. Liu, and P. Deng, "Odor recognition in multiple E-Nose systems with cross-domain discriminative subspace learning," *IEEE Trans. Instrum. Meas.*, vol. 66, no. 7, pp. 1679–1692, Jul. 2017.

[24] B. Liu, X. Zeng, F. Tian, S. Zhang, and L. Zhao, "Domain transfer broad learning system for long-term drift compensation in electronic nose systems," *IEEE Access*, vol. 7, pp. 143947–143959, 2019.

[25] Y. Tian *et al.*, "A drift-compensating novel deep belief classification network to improve gas recognition of electronic noses," *IEEE Access*, vol. 8, pp. 121385–121397, 2020.

[26] J. X. Leon-Medina, W. A. Pineda-Munoz, and D. A. Tibaduiza, "Joint distribution adaptation for drift correction in electronic nose type sensor arrays," *IEEE Access*, vol. 8, pp. 134413–134421, 2020.

[27] A. Ur Rehman and A. Bermak, "Drift-insensitive features for learning artificial olfaction in E-Nose system," *IEEE Sensors J.*, vol. 18, no. 17, pp. 7173–7182, Sep. 2018.
[28] S. De Vito, G. Fattoruso, M. Pardo, F. Tortorella, and G. Di Francia, "Semi-supervised learning techniques in artificial olfaction: A novel approach to classification problems and drift counteraction," *IEEE Sensors J.*, vol. 12, no. 11, pp. 3215–3224, Nov. 2012.
[29] X. Pan, H. Zhang, W. Ye, A. Bermak, and X. Zhao, "A fast and robust gas recognition algorithm based on hybrid convolutional and recurrent neural network," *IEEE Access*, vol. 7, pp. 100954–100963, 2019.
[30] A. Vergara, S. Vembu, T. Ayhan, M. A. Ryan, M. L. Homer, and R. Huerta, "Chemical gas sensor drift compensation using classifier ensembles," *Sens. Actuators B, Chem.*, vols. 166–167, pp. 320–329, May 2012.
[31] D. R. Wijaya and F. Afianti, "Stability assessment of feature selection algorithms on homogeneous datasets: A study for sensor array optimization problem," *IEEE Access*, vol. 8, pp. 33944–33953, 2020.
[32] A. U. Rehman, A. Bermak, and M. Hamdi, "Shuffled frog-leaping and weighted cosine similarity for drift correction in gas sensors," *IEEE Sensors J.*, vol. 19, no. 24, pp. 12126–12136, Dec. 2019.
[33] A. U. Rehman and A. Bermak, "Recursive DBPSO for computationally efficient electronic nose system," *IEEE Sensors J.*, vol. 18, no. 1, pp. 320–327, Jan. 2018.
[34] A. ur Rehman and A. Bermak, "Swarm intelligence and similarity measures for memory efficient electronic nose system," *IEEE Sensors J.*, vol. 18, no. 6, pp. 2471–2482, Mar. 2018.
[35] K. Yan, L. Kou, and D. Zhang, "Learning domain-invariant subspace using domain features and independence maximization," *IEEE Trans. Cybern.*, vol. 48, no. 1, pp. 288–299, Jan. 2018.
[36] L. Zhang and D. Zhang, "Domain adaptation extreme learning machines for drift compensation in E-Nose systems," *IEEE Trans. Instrum. Meas.*, vol. 64, no. 7, pp. 1790–1801, Jul. 2015.
[37] L. Zhang, D. Zhang, X. Yin, and Y. Liu, "A novel semi-supervised learning approach in artificial olfaction for E-Nose application," *IEEE Sensors J.*, vol. 16, no. 12, pp. 4919–4931, Jun. 2016.

Atiq Ur Rehman (Member, IEEE) received the master's degree in computer engineering from the National University of Sciences and Technology (NUST), Pakistan, in 2013, and the Ph.D. degree in computer science and engineering from Hamad Bin Khalifa University, Qatar, in 2019. He is currently working as a Postdoc Researcher with the College of Science and Engineering, Hamad Bin Khalifa University. His research interests include the development of evolutionary computation, pattern recognition, and machine learning algorithms.

Samir Brahim Belhaouari (Senior Member, IEEE) received the master's degree in telecommunications from the National Polytechnic Institute (ENSEEIHT) of Toulouse, France, in 2000, and the Ph.D. degree in applied mathematics from the Federal Polytechnic School of Lausanne (EPFL) in 2006. He is currently an Associate Professor with the Division of Information and Computing Technology, College of Science and Engineering, HBKU. He also holds and leads several academic and administrator positions, Vice Dean for Academic and Student Affairs at the College of Science and General Studies and University Preparatory Program at ALFAISAL University (KSA), University of Sharjah (UAE), Innopolis University (Russia), Petronas University (Malaysia), and EPFL Federal Swiss School (Switzerland). His main research interests include stochastic processes, machine learning, and number theory. He is now working actively on developing algorithms in machine learning applied to visual surveillance, sensing technologies and biomedical data, with the support of several international fund for research in Russia, Malaysia, and in GCC.

Muhammad Ijaz received the master's degree in computer engineering form the King Fahad University of Petroleum and Minerals (KFUPM), KSA. He is currently pursuing the Ph.D. degree in computer science and engineering from Hamad Bin Khalifa University, Doha, Qatar. His research interests include development of machine learning algorithms for sensing technologies and the IoT.

Amine Bermak (Fellow, IEEE) received the M.Eng. and Ph.D. degrees in electronic engineering from Paul Sabatier University, Toulouse, France, in 1994 and 1998, respectively. He was with the French National Research Center, Microsystems and Microstructures Research Group, LAAS-CNRS, where he developed a 3-D VLSI chip for artificial neural network classification and detection applications. He joined the Advanced Computer Architecture Research Group, York University, York, U.K., where he held a post-doctoral position on VLSI implementation of CMM neural network for vision applications in a project funded by the British Aerospace. In 1998, he joined Edith Cowan University, Perth, Australia, as a Research Fellow in smart vision sensors, and a Senior Lecturer with the School of Engineering and Mathematics. He served as a Professor with the Electronic and Computer Engineering Department, The Hong Kong University of Science and Technology, where he was also serving as the Director of Computer Engineering and the Director of the M.Sc. degree program in integrated circuit design. He is currently a Professor and an Associate Dean with the College of Science and Engineering, Hamad Bin Khalifa University, Qatar. His research interests include VLSI circuits and systems for signal, image processing, sensors, and microsystem applications.

Mounir Hamdi (Fellow, IEEE) received the B.S. (Hons.) degree in electrical engineering (minor in computer engineering) from the University of Louisiana in 1985 and the M.S. and Ph.D. degrees in electrical engineering from the University of Pittsburgh in 1987 and 1991, respectively. He is currently the Dean of the College of Science and Engineering, Hamad Bin Khalifa University (HBKU). Before joining HBKU, he was a Chair Professor with the Hong Kong University of Science and Technology (HKUST), and the Head of the Department of Computer Science and Engineering. Prof. Hamdi is/was on the Editorial Board of various prestigious journals and magazines including the IEEE TRANSACTIONS ON COMMUNICATIONS, *IEEE Communication Magazine, Computer Networks, Wireless Communications and Mobile Computing, and Parallel Computing* as well as a Guest Editor of *IEEE Communications Magazine*, the Guest Editor-In-Chief of two special issues of the IEEE JOURNAL ON SELECTED AREAS OF COMMUNICATIONS, and a Guest Editor of *Optical Networks Magazine*.